

## Multi-Wave Mixing in Potassium Vapour

Maohong Lu ( 陸懋宏 ), Kunwei Lin ( 林焜尉 )  
and Juinhuei Tsai ( 蔡君徽 )

*Institute of Electra-optical Engineering, National Chiao Tung University*  
*Hsinchu, Taiwan, R.O.C.*

(Received October 19, 1987)

Four-wave and six-wave mixing processes under two-photon transitions (4S-8S), (4S-7S), (4S-6D) and (4S-5D) in potassium vapour have been investigated for the wavelength range 300-370nm. The wave-coupling schemes and the non-collinear phase-match angles for the observed UV lines have been analyzed. Frequency doubling under resonant and near-resonant conditions has been observed.

### INTRODUCTION

The nonlinear optical properties of alkali metal vapours have received considerable attention recently. They have the potential to serve as sources of coherent radiation over a spectral range which extends from the ultra-violet to the far infra-red. Under resonant conditions, a high nonlinear susceptibility and a high conversion efficiency may be obtained. By using two-photon resonances in sodium<sup>1</sup>, potassium\*, and cesium<sup>3</sup>, some coherent  $\mathbf{W}$  emissions through four or six-wave-mixing processes have been observed.

In this paper we describe the generation of coherent UV radiation lines in the wavelength range 300-370nm by two-photon resonances ( $4^2 S_{1/2} - 8^2 S_{1/2}$ ), ( $4^2 S_{1/2} - 7^2 S_{1/2}$ ), ( $4^2 S_{1/2} - 6^2 D_{3/2, 5/2}$ ), ( $4^2 S_{1/2} - 5^2 D_{3/2, 5/2}$ ), etc. These coherent  $\mathbf{W}$  radiation lines are produced by four-wave and six-wave mixing processes. In these processes, two laser photons are mixed with one or three IR photons to produce a UV photon. The intensities of the resultant UV lines depend strongly on some resonant or near resonant enhancements in the intermediate processes. For the two-photon resonance (4S-8S), we compare the results of this work with Zhang et al's results.<sup>2</sup>

We have also observed the frequency-doubled radiations, which appear at two-photon resonant pumping wavelengths and near-resonant wavelengths.

## II. EXPERIMENTAL SETUP

The experimental setup is shown in Fig. 1. A tunable pulsed dye laser (Quanta-Ray, PDL-1) pumped by a frequency-doubled Nd:YAG laser (JK Lasers, HY750) was used as the pumping source, operating at 10Hz. Using DCM dye, the wavelength can be tuned to 605-670 nm with a linewidth of 10GHz. The laser's output energy was 5-7 mJ per pulse. The duration of the laser pulse was about 25ns.

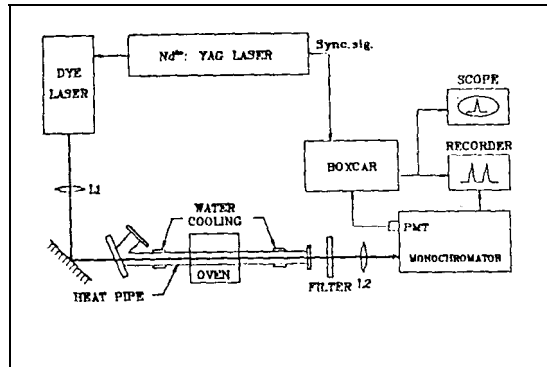


FIG. 1 Experimental setup.

Potassium vapour was produced in a heat pipe oven<sup>11</sup> made from a stainless-steel tube and heated to a temperature of 350-400°C. The heat pipe was 90cm long and 3.6cm in diameter, with a heating region of 30 cm. It was operated between 35 and 40 torr using helium as the buffer gas. The output radiation was filtered against the pumping light with a filter (Melles Griot UG11), and was detected by a photomultiplier (Hamamasu R928) after a 1-m monochromator (Spex 1704) with 50 $\mu$ m slits. The wavelength accuracy measured in this experiment is about 0.05nm. The monochromator was calibrated using the emission lines of a mercury lamp and a He-Ne laser. The output current from the photomultiplier was fed directly into a boxcar (NF BX53 1). The results were plotted by a chart recorder.

The laser beam was focussed into the center of the heat pipe oven using an 80cm focal-length lens. The spot diameter was about 0.3mm. The output light was passed through the filter and then focused by a quartz lens onto the entrance slit of the monochromator.

## III. RESULTS AND DISCUSSION

When focussing a laser beam into the potassium vapour and tuning it resonant to the two-photon transitions of the potassium atoms, three different multi-wave coupling processes are of particular interest with respect to the generation of coherent UV radiation: (1) coupling of two laser photons with one IR photon from optically pumped, stimulated IR

transitions or other IR generation mechanisms,  $\omega_{uv} = 2\omega_L \pm \omega_{IR}$  (four-wave mixing), (2) coupling of two laser photons with three IR photons from laser induced, stimulated IR transitions  $\omega_{uv} = 2\omega_L - \omega_{IR} - \omega'_{IR} \pm \omega''_{IR}$  (six-wave mixing), and (3) direct coupling of two laser photons (frequency doubling). The last process is forbidden in the electric-dipole approximation for a centro-symmetric medium, but it can be generated due to a laser induced dc-electric field.<sup>6,8</sup>

If the laser is tuned to the two-photon transitions (4S-8S), (4S-7S), (4S-6D) and (4S-5D), respectively 27, 23, 28 and 18 lines in the wavelength range 300-370nm have been observed, see tables 1, 2, 3, and 4. The output UV radiation is so strong that it can be observed on a white paper put in front of the entrance slit of the monochromator.

(1) IR photon generations:

In these multi-wave mixing processes, IR radiations could be generated in many ways: (a) optically pumped stimulated emission (OPSE), (b) stimulated electronic hyper-Raman scattering (SEMRS), (c) stimulated electric Raman scattering (SERS), and (d) parametric process.

Suppose that only one mechanism of IR generation and only one multiwave-mixing process is dominant, and that the IR wave energy increases exponentially in the propagation direction of the laser beam:

$$E_{IR}^{(i)}(z) = E_{IR}^{(i)}(0)e^{g_i z/2} \quad (1)$$

where  $g_i$  is the gain of the  $i$ th IR wave.

The wave equation for the UV radiation can then be solved with some approximations. The relation of the UV light intensity to the IR wave gain can be expressed by

$$I_{uv} \sim \frac{1}{[g_{IR}^2 + (\Delta k)^2]} \quad (2)$$

where for four-wave mixing processes,  $g_{IR} = g_i$  is the gain of the involved IR wave and  $\Delta k = 2k_L \pm k_{IR} - k_{uv}$  is the collinear phase mismatch; for six-wave mixing processes,  $g_{IR} = g'_{IR} + g''_{IR} + g'''_{IR}$ , which are the gains of the different IR waves involved and  $\Delta k = 2k_L - k_{IR} - k''_{IR} \pm k'''_{IR} - k_{uv}$  is the collinear phase mismatch.

From Equ. (2), if  $|\Delta k| \ll g_{IR}$ , then  $\Delta k$  can be ignored, and in this case, the collinear phase mismatch is not important.

The quantitative determination of the contributions of the above mentioned processes to the generation of the IR waves requires a systematic investigation of its dependence on the laser power and the detuning from resonances.

(2) Four-wave mixing processes

The energy level diagram of potassium is shown in Fig. 2.<sup>7,9</sup> In the two-photon

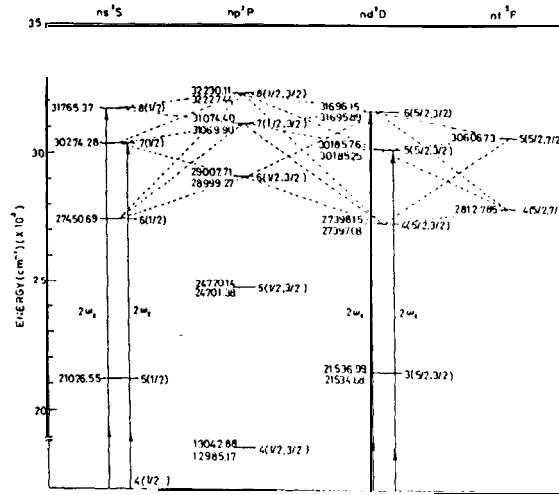


FIG. 2 The energy levels of potassium.

resonances ( $4S-8S$ ) and ( $4S-6D$ ), the two strongest lines are observed at 321.7nm and 344.6 nm. They are produced by two laser photons mixing with an IR photon from laser induced, stimulated emission. In the ( $4S-8S$ ) resonance, the IR photons are ( $8^2S_{1/2}, 7^2P_{3/2}$ ) and ( $8^2S_{1/2}, 6^2P_{3/2}$ ) respectively for the two lines. In the ( $4S-6D$ ) resonance, the IR photons are ( $6^2D_{3/2, 5/2}, 7^2P_{3/2}$ ) and ( $6^2D_{3/2, 5/2}, 6^2P_{3/2}$ ) respectively for the two lines. In the two-photon resonances ( $4S-7S$ ) and ( $4S-5D$ ), only one strong line was observed at 344.6nm—this line is also due to the four-wave mixing process. For the ( $4S-7S$ ) and ( $4S-5D$ ) cases, the IR photons are ( $7^2S_{1/2}, 6^2P_{3/2}$ ) and ( $5^2D_{3/2, 5/2}, 6^2P_{3/2}$ ), respectively.

Since many IR photons with different wavelengths exist, as mentioned above, many lines produced by four-wave mixing processes have been observed. The relative intensities and coupling schemes for each line are listed in Table 1, 2, 3 and 4 where the line intensities have not been corrected for the spectral responsivity of the PMT. The line intensities depend strongly on the resonant or near-resonant enhancements. Three typical coupling schemes for four-wave mixing are shown in Fig. 3.

### (3) Six-wave mixing processes

A six-wave mixing process is a fifth-order process, which is formed by the coupling of two laser photons with three IR photons. In general, the coherent UV radiation can be expressed by  $\omega_{uv} = 2\omega_L - \omega'_{IR} - \omega''_{IR} \pm \omega'''_{IR}$  and the relative intensities of six-wave mixing processes should be weaker than those of four-wave mixing processes. We find 18 lines formed by six-wave mixing for the ( $4S-8S$ ) two-photon resonance, 17 lines for the ( $4S-7S$ ), 22 lines for the ( $4S-6D$ ), and 15 lines for the ( $4S-5D$ ), see Tables 1, 2, 3 and 4. Since the power of our pumping laser is much stronger than that used in Zhang et al.'s work, we get an extra 13 lines for the ( $4S-8S$ ) two-photon resonance in the wavelength range 300-370 nm. Some typical coupling schemes for six-wave mixing are shown in Fig. 4. There are two similar processes are shown in Fig. 4(b) and 4(c). The one in Fig. 4(b) is enhanced by a

TABLE 1. Wavelength, Intensity, and Coupling Scheme of W Lines under (4S, 8S) Two Photon Resonance

$2u_1$ (8S, 4S) $\lambda$ (nm)	Pumping Wavelength=629.46 (nm) Relative Intensity	Theoretical $\lambda$ (nm)	Coupling Scheme	Characteristics	
				Resonances	Near-resonances
303.52	352	303.48	$2u_1 + u(3D, 6P)$	onefold	onefold, $d=0.3\text{cm}^{-1}$
308.06	115	308.04	$2u_1 + u(8S, 7P)$	onefold	onefold, $d=225.2\text{cm}^{-1}$
308.65	95	308.60	$2u_1 - u(8S, 6P) + u(8S, 7P) + u(4D, 5P)$	twofold	twofold, $d_1=166.8\text{cm}^{-1}, d_2=62\text{cm}^{-1}$
313.05	79	313.04	$2u_1 - 2u(8S, 7P) + u(6P, 6S)$	twofold	twofold, $d_1=297.5\text{cm}^{-1}$ $d_2=109.8\text{cm}^{-1}$
317.40	136	317.40	$2u_1 - u(8S, 7P) + u(5P, 3D) - u(8S, 6P)$	twofold	onefold, $d=36\text{cm}^{-1}$
321.71	1940	321.71	$2u_1 - u(8S, 7P)$	twofold	
322.90	506	322.86	$2u_1 - u(7P, 7S)$	onefold	onefold, $d=109\text{cm}^{-1}$
323.80	317	323.78	$2u_1 - u(7P, 5D)$	onefold	onefold, $d=199\text{cm}^{-1}$
325.76	210	325.75	$2u_1 - u(8S, 7P) + u(7P, 7S) - u(5D, 6P)$	twofold	onefold, $d=110\text{cm}^{-1}$
326.08	215	326.10	$2u_1 - u(8S, 7P) + u(6S, 5P) - u(5P, 3D)$	twofold	onefold, $d=27.2\text{cm}^{-1}$
334.80	141	334.82	$2u_1 - u(8S, 7P) + u(6P, 6S) - u(8S, 6P)$	twofold	onefold, $d=24.8\text{cm}^{-1}$
338.95	337	338.95	$2u_1 - 2u(8S, 7P) - u(7P, 5D)$	threefold	
339.22	153	339.19	$2u_1 - u(8S, 7P) - 2u(7P, 7S)$	threefold	
340.21	188	340.21	$2u_1 - u(8S, 7P) - u(7P, 7S) - u(7P, 5D)$	threefold	
341.25	106	341.25	$2u_1 - u(8S, 7P) - 2u(7P, 5D)$	threefold	onefold, $d=288\text{cm}^{-1}$
342.25	53	342.27	$2u_1 - u(8S, 7P) - u(7P, 6S) - u(5D, 5P)$	twofold	twofold, $d_1=1.4\text{cm}^{-1}, d_2=206.4\text{cm}^{-1}$
343.60	223	343.59	$2u_1 - u(8S, 7P) - u(7P, 7S) - u(5D, 6P)$	threefold	onefold, $d=89\text{cm}^{-1}$
344.05	129	344.05	$2u_1 - u(8S, 7P) + u(6P, 4D) - u(7P, 6S)$	twofold	twofold, $d_1=27.8\text{cm}^{-1}, d_2=48.7\text{cm}^{-1}$
344.36	290	344.33	$2u_1 - u(6S, 5P)$	onefold	onefold, $d=26.8\text{cm}^{-1}$
344.65	1000	344.65	$2u_1 - u(8S, 6P)$	twofold	
345.75	294	345.78	$2u_1 - u(8S, 7P) - u(7P, 5D) - u(7S, 6P)$	threefold	onefold, $d=4\text{cm}^{-1}$
347.82	140	347.90	$2u_1 - u(8S, 6P) + u(7S, 6P) - u(6P, 6S)$	twofold	twofold, $d_1=8.67\text{cm}^{-1}, d_2=273.7\text{cm}^{-1}$
348.16	158	348.16	$2u_1 - u(8S, 7P) + u(7P, 7S) - u(5P, 3D)$	twofold	twofold, $d_1=110\text{cm}^{-1}, d_2=294\text{cm}^{-1}$
357.00	64	357.01	$2u_1 - u(8S, 6P) + u(4D, 5P) - u(5P, 5S)$	twofold	onefold, $d=10.8\text{cm}^{-1}$
357.28	129	357.30	$2u_1 - u(8S, 6P) + u(4D, 5P) - u(5P, 5S)$	twofold	onefold, $d=10.8\text{cm}^{-1}$
314.72	22		S.H.G		
341.66	53		Not Found		

\*This line has been observed by Zhang, etc. [2]

TABLE 2. Wavelength, Intensity, and Coupling Scheme of *W Lines* under (4S, 7S) Two Photon Resonance

$2u_1$ (7S, 4S) $\lambda$ (nm)	Pumping Wavelength=660.49 (nm) Relative Intensity	Theoretical $\lambda$ (nm)	Coupling Scheme	Characteristics	
				Resonances	Near-resonances
301.60	27	301.58	$2u_1 - u(6P, 6S) + u(7S, 6P) + u(5P, 3D)$	onefold	threefold, $d_1=27.5\text{cm}^{-1}$ $d_2=5.0\text{cm}^{-1}, d_3=206\text{cm}^{-1}$
306.80	26	306.42	$2u_1 - u(6P, 4D) - u(6P, 4D) + u(7S, 5P)$	onefold	threefold, $d_1=12\text{cm}^{-1}, d_2=315\text{cm}^{-1}$ $d_3=344.4\text{cm}^{-1}$
316.65	57	316.62	$2u_1 - u(6P, 6S) - u(4D, 5P) + u(7S, 5P)$	onefold	twofold, $d_1=49\text{cm}^{-1}, d_2=290.8\text{cm}^{-1}$
316.95	21	316.89	$2u_1 + u(7S, 6P)$	onefold	
321.00	53	320.97	$2u_1 - u(7S, 5P) - u(6P, 5S) + u(6S, 4P)$	twofold	onefold, $d=72.3\text{cm}^{-1}$
321.60	88	321.56	$2u_1 - u(7S, 6P) - u(6P, 4D) + u(5P, 5S)$	threefold	onefold, $d=16\text{cm}^{-1}$
322.22	14	322.16	$2u_1 - u(7S, 5P) - u(6S, 4P) + u(4D, 4P)$	twofold	onefold, $d=42\text{cm}^{-1}$
330.60	74	330.60	$2u_1 - u(6P, 4D) - u(6P, 4D) + u(5P, 5S)$	onefold	twofold, $d_1=48.5\text{cm}^{-1}, d_2=84\text{cm}^{-1}$
331.70	65	331.23	$2u_1 - u(7S, 5P) + u(6P, 6S) + u(6S, 5P)$	threefold	
335.35	68	335.34	$2u_1 - u(6P, 4D) - u(6P, 6S) + u(4D, 5P)$	onefold	twofold, $d_1=28.8\text{cm}^{-1}, d_2=273.7\text{cm}^{-1}$
339.75	131	339.76	$2u_1 - u(7S, 6P) - u(6S, 5P) + u(5P, 3D)$	twofold	
344.55	1000	344.65	$2u_1 - u(7S, 6P)$	twofold	
345.70	186	345.62	$2u_1 - u(7S, 6P) + u(4D, 5P) - u(6S, 5P)$	twofold	twofold, $d_1=19.6\text{cm}^{-1}, d_2=72.4\text{cm}^{-1}$
347.45	81	347.47	$2u_1 - u(6P, 6S) - u(6P, 6S) + u(6P, 4D)$	onefold	threefold, $d_1=273.7\text{cm}^{-1}, d_2=52.5\text{cm}^{-1}$ $d_3=229.6\text{cm}^{-1}$
348.00	272	348.00	$2u_1 - u(6P, 6S)$	onefold	onefold, $d=273.7\text{cm}^{-1}$
348.78	249	348.75	$2u_1 - u(6P, 4D)$	onefold	onefold, $d=335.8\text{cm}^{-1}$
349.20	128	349.19	$2u_1 - u(6P, 4D) + u(4D, 5P) - u(6S, 5P)$	onefold	twofold, $d_1=28.8\text{cm}^{-1}, d_2=33.8\text{cm}^{-1}$
353.95	93	353.92	$2u_1 - u(6P, 4D) + u(6S, 5P) - u(5P, 3D)$	onefold	twofold, $d_1=0.3\text{cm}^{-1}, d_2=282.8\text{cm}^{-1}$
357.13	71	357.13	$2u_1 - u(7S, 6P) + u(4D, 5P) - u(5P, 5S)$	twofold	onefold, $d=9.9\text{cm}^{-1}$
357.25	74	357.25	$2u_1 - u(7S, 6P) + u(4D, 5P) - u(5P, 5S)$	twofold	onefold, $d=18.5\text{cm}^{-1}$
362.95	105	362.95	$2u_1 - u(7S, 6P) + u(6P, 6S) - u(4D, 5P)$	twofold	onefold, $d=282.1\text{cm}^{-1}$
330.20	26		S.H.G		

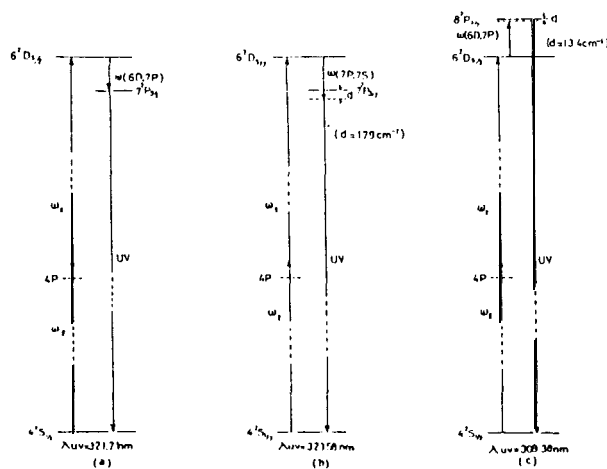
threefold resonance, the other in Fig. 4(c) is enhanced by a threefold resonance and a one-fold near resonance. Obviously, the intensity of the latter should be much stronger than that of the former. The coupling scheme of six-wave mixing process for every particular UV line is also listed in Tables 1, 2, 3, and 4. In the analysis of these six-wave mixing processes, we have noticed that there may be more than one coupling scheme available to produce a particular line, as shown in Fig. 5, but only one scheme is listed in Tables. The scheme listed has the minimum offset from resonance and the best phase matching.

**TABLE 3.** Wavelength, Intensity, and Coupling Scheme of UV Lines under (4S, 6D) Two Photon Resonance

$2u_1$ (6D, 4S) $\lambda$ (nm)	Pumping Wavelength=630.83 (nm)		Coupling Scheme	Characteristics	
	Experimental Intensity	Theoretical		Resonances	Near-resonances
308.68	141	308.62	$2u_1 - u(6D, 5F) - u(7P, 5D) + u(4D, 5P)$	twofold	twofold, $d_1=105.3\text{cm}^{-1}$ , $d_2=64\text{cm}^{-1}$
309.38	147	309.35	$2u_1 + u(6D, 7P)$	onefold	onefold, $d=13.4\text{cm}^{-1}$
313.05	171	313.02	$2u_1 - u(6D, 6P) - u(4D, 4P) + u(7S, 4P)$	twofold	onefold, $d=285.6\text{cm}^{-1}$
317.35	225	317.35	$2u_1 - u(6D, 6P) - u(5D, 6P) + u(7P, 4D)$	twofold	onefold, $d=31.6\text{cm}^{-1}$
319.40	384	319.42	$2u_1 - u(6D, 5F) + u(6S, 5P) - u(5D, 4F)$	twofold	twofold, $d_1=217.4\text{cm}^{-1}$ , $d_2=222.7\text{cm}^{-1}$
321.71	6480		$2u_1 - u(6D, 7P)$	twofold	
323.58	396	323.58	$2u_1 - u(7P, 7S)$	onefold	onefold, $d=174.5\text{cm}^{-1}$
330.48	192	330.49	$2u_1 - u(6D, 7P) - u(6P, 6S) + u(4F, 4D)$	twofold	onefold, $d=40.2\text{cm}^{-1}$
337.15	180	337.14	$2u_1 - u(6D, 7P) + u(7S, 6P) - u(4D, 5P)$	twofold	onefold, $d=248.8\text{cm}^{-1}$
337.23	132	337.28	$2u_1 - u(5D, 4F)$	onefold	
338.64	144	338.64	$2u_1 - u(6D, 7P) + u(5D, 6P) - u(6S, 5P)$	onefold	twofold, $d_1=67.2\text{cm}^{-1}$ , $d_2=42.6\text{cm}^{-1}$
339.20	214	339.20	$2u_1 - u(6D, 6P) - u(6D, 7P) + u(6D, 5F)$	twofold	onefold, $d=87.5\text{cm}^{-1}$
340.22	144	340.22	$2u_1 - u(6D, 7P) - u(7P, 7S) - u(7P, 5D)$	threefold	
344.66	1000		$2u_1 - u(6D, 6P)$	twofold	
345.92	195	345.92	$2u_1 - u(6D, 7P) - u(6P, 6S)$	twofold	twofold, $d_1=179.5\text{cm}^{-1}$ , $d_2=94.2\text{cm}^{-1}$
348.00	270	348.00	$2u_1 - u(6D, 7P) + u(5F, 4D) - u(7S, 5P)$	twofold	twofold, $d_1=49.3\text{cm}^{-1}$ , $d_2=270.2\text{cm}^{-1}$
348.12	234	348.12	$2u_1 - u(6D, 7P) - u(7P, 7S) - u(6P, 6S)$	threefold	onefold, $d=282\text{cm}^{-1}$
348.80	123	348.78	$2u_1 - u(6D, 7P) - u(7P, 7S) - u(6P, 4D)$	threefold	onefold, $d=335.7\text{cm}^{-1}$
352.40	138	352.40	$2u_1 - u(6D, 6P) - u(6D, 6P) + u(5D, 4F)$	twofold	
353.49	132	353.41	$2u_1 - u(6D, 5F) - u(5F, 4D) + u(7P, 5D)$	threefold	
357.49	234	357.42	$2u_1 - u(6D, 7P) - u(6P, 6S) - u(6P, 6S)$	twofold	
358.71	120	358.71	$2u_1 - u(6D, 7P) - u(7P, 6S) + u(5F, 5D)$	threefold	
359.40	111	359.39	$2u_1 - u(6D, 7P) - u(7P, 4D) + u(5F, 5D)$	threefold	
363.14	123	363.14	$2u_1 - u(6D, 6P) + u(6P, 6S) - u(5P, 3D)$	twofold	onefold, $d=290.8\text{cm}^{-1}$
365.45	147	365.45	$2u_1 - u(6D, 6P) - u(5F, 4D) + u(6P, 6S)$	twofold	onefold, $d=290.8\text{cm}^{-1}$
369.38	96	369.49	$2u_1 - u(6D, 5F) + u(7P, 7S) - u(6S, 5P)$	twofold	
	103	369.81	$2u_1 - u(6D, 7P) - u(7P, 6S) - u(5F, 5D)$	threefold	
315.12	25		S.H.G		

**TABLE 4.** Wavelength, Intensity, and Coupling Scheme of UL Lines under (4S, 5D) Two Photon Resonance

$2u_1$ (5D, 4S) $\lambda$ (nm)	Pumping Wavelength=662.44 (nm)		Coupling Scheme	Characteristics	
	Experimental Intensity	Theoretical		Resonances	Near-resonances
306.78	27	306.73	$2u_1 - u(5D, 5P) - u(4F, 3D) + u(5S, 4P)$	twofold	
316.10	53	316.02	$2u_1 - u(5D, 5P) - u(6P, 6S) + u(5D, 4P)$	twofold	onefold, $d=14.7\text{cm}^{-1}$
320.88	68	320.86	$2u_1 - u(5D, 5P) - u(6P, 4D) + u(5S, 4P)$	twofold	twofold, $d_1=113.5\text{cm}^{-1}$ , $d_2=86\text{cm}^{-1}$
321.20	24	321.20	$2u_1 - u(5D, 6P) - u(6P, 6S) + u(5P, 5S)$	threefold	onefold, $d=51.8\text{cm}^{-1}$
321.54	20	321.45	$2u_1 - u(5D, 6P) - u(6P, 4D) + u(5P, 5S)$	twofold	twofold, $d_1=9.8\text{cm}^{-1}$ , $d_2=25.5\text{cm}^{-1}$
321.60	25	321.55	$2u_1 - u(5D, 4F) - u(4F, 4D) + u(5P, 5S)$	threefold	onefold, $d=16\text{cm}^{-1}$
321.81	29	321.75	$2u_1 - u(5D, 4F) - u(4F, 4D) + u(5P, 5S)$	threefold	onefold, $d=1.7\text{cm}^{-1}$
330.25	95	330.33	$2u_1 - u(5D, 4F) - u(6P, 6S) + u(5P, 5S)$	twofold	onefold, $d=56.2\text{cm}^{-1}$
331.23	53	331.17	$2u_1 - u(5D, 6P) - u(6P, 6S) + u(5P, 5S)$	threefold	
			S.H.G		
335.10	92	335.09	$2u_1 - u(5D, 6P) - u(4F, 4D) + u(6P, 6S)$	twofold	onefold, $d=291\text{cm}^{-1}$
339.85	115	339.87	$2u_1 - u(5D, 6P) - u(6S, 5P) + u(5P, 3D)$	twofold	
342.95	153	342.87	$2u_1 - u(6P, 6S) - u(6P, 6S) + u(5D, 4P)$	onefold	onefold, $d=141.4\text{cm}^{-1}$
344.66	1000	344.66	$2u_1 - u(5D, 6P)$	twofold	
346.60	107	346.64	$2u_1 - u(5D, 5P) + 2u(5D, 4F)$	twofold	onefold, $d=164\text{cm}^{-1}$
349.15	153	349.15	$2u_1 - u(6P, 6S)$	onefold	
356.42	49	356.46	$2u_1 - u(5D, 6P) + u(6P, 4D) - u(6S, 5P)$	twofold	onefold, $d=344.2\text{cm}^{-1}$
363.00	27	363.01	$2u_1 - u(5D, 4F) + u(6S, 5P) - u(5P, 5S)$	twofold	
306.25	55		Not Found.		

**FIG. 3** Coupling schemes of three Four-wave mixing processes for (a) line 321.71nm, (b) line 323.58nm and (c) line 309.38nm.

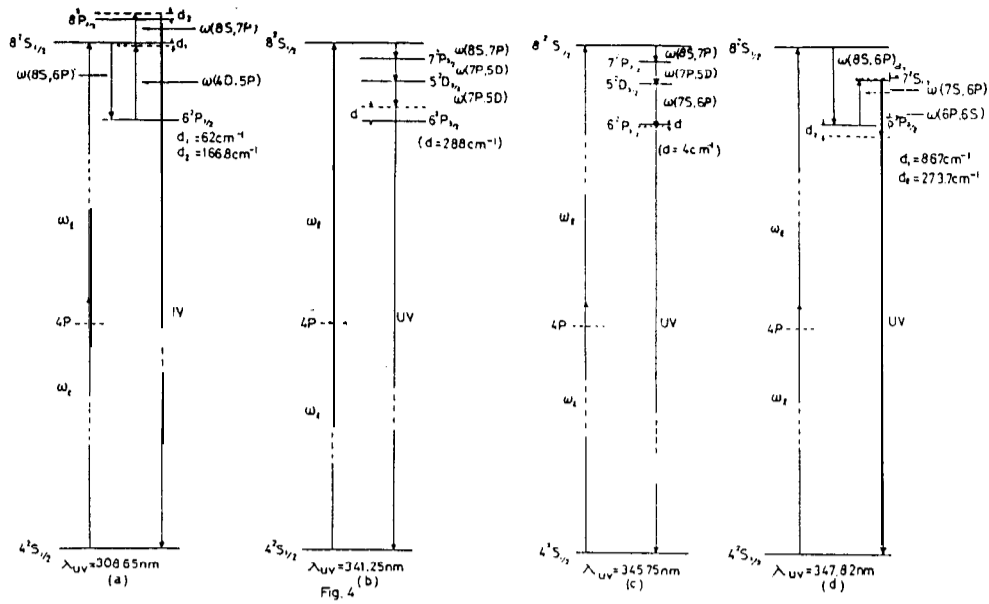


FIG. 4 Three typical coupling schemes of six-wave mixing processes for (a) line 308.65nm, (b) line 341.25nm (c) line 345.75nm and (d) line 347.82nm.

(4) Phase match

As mentioned before, the phase mismatch  $\Delta k$  is non-critical for maximum conversion if

$$4(\Delta k^2 / g^2_{\text{IR}}) \ll 1 \quad (3)$$

This condition may be replaced by a less rigorous one. In our case a focused laser beam is used, so non-collinear phase-match is possible. Considering two of the coupling waves to be collinear and calculating the angle between the two other waves, as shown in Fig. 6, one obtains for the two coupling cases:

(a) UV and IR waves are collinear,  $k_{\text{uv}} \parallel \Sigma k_{\text{IR}}$ ,

$$\cos \psi = \frac{k_{\text{uv}} + k_{\text{IR}}}{2 k_L} \quad (4)$$

where  $k_{\text{IR}}$  is the total wave vector of the IR waves involved in the mixing process. We assume that all the IR wave vectors are collinear, so  $|\Sigma k_{\text{IR}}| = k'_{\text{IR}} + k''_{\text{IR}} \pm k'''_{\text{IR}}$ .

MULTI-WAVE MIXING IN POTASSIUM VAPOUR

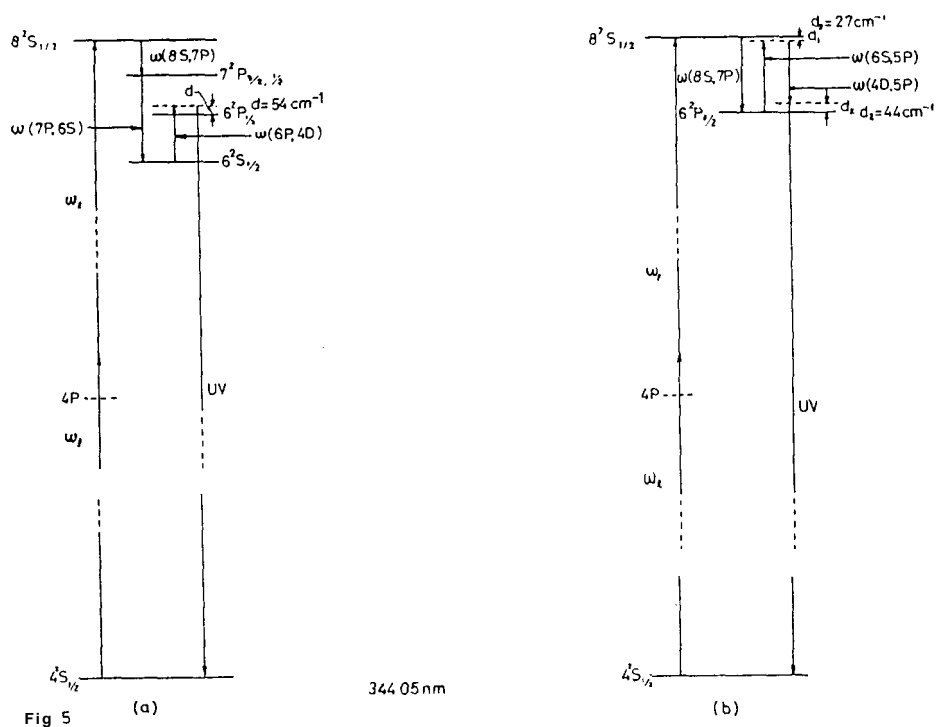


FIG. 5 Two coupling schemes are possible to produce the line 344.05nm.

(b) two laser waves are collinear, we have

$$\cos \phi = \frac{k_{uv}^2 + 4k_L^2 - |\Sigma k_{IR}|^2}{4k_{uv}k_L} \quad (5)$$

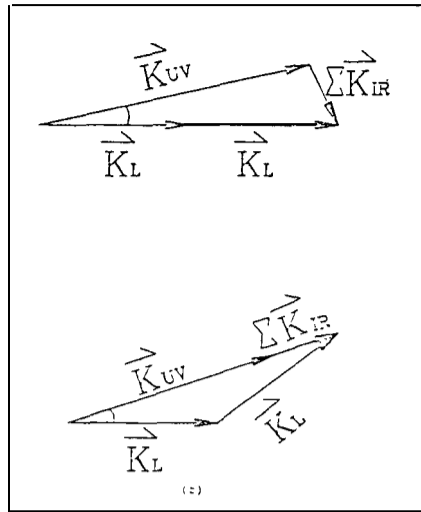
k is defined by  $\frac{\omega}{c} n(\omega)$ , where n is the refractive index at the wave number  $\omega$ . n( $\omega$ ) of potassium vapour can be calculated using the Sellmeier equation,

$$n(\omega) - 1 = \frac{Nr_e}{2\pi} \sum_n \frac{f_{np}}{\omega_{np}^2 - \omega^2}, \quad n \geq 4 \quad (6)$$

where  $r_e = 2.818 \times 10^{-13}$  cm,  $\omega_{np}$  is the energy of the np level in wave number,  $N \cong 10^{16}$  / cm<sup>3</sup> is the potassium density at temperature 350°C, and  $f_{np}$  is the oscillator strength of the transition from np to 4s<sup>5</sup>. The phase match angle  $\psi$  or  $\phi$  for each line is shown in Tables 5, 6, 7, and 8. From these tables, all the phase match angles are very small, so the phase matching conditions are easily satisfied for our diverging laser beam.

(5) Frequency doubling

Under two-photon resonances (4S-8S), (4S-7S), (4S-6D) and (4S-5D), the frequency



IFG FIG. 6 Two coupling cases for phase matching.

doubling ( $\omega_{UV} = 2\omega_L$ ) has been observed and the spectra are shown in Fig. 7. We have also observed the frequency doubling under near two-photon resonances. The frequency doubling output as a function of wavelength near the (4S-7S) resonance was measured, as

FIG. 5 Noncollinear Phase Matching Angles for Each W Lines Under (4S,8S) Two-Photon Resonance

FIG. 6 Noncollinear Phase Matching Angles for Each W Lines Under(4S,7S) Two-photon Resonance

Experimental (nm) $\lambda$	Phase Matching Angle (urad)		Experimental (nm) $\lambda$	Phase Matching Angle (urad)	
	$\psi$	$\phi$		$\psi$	$\phi$
303.52	3.3		301.60	2.4	
308.06	2.6		306.80	6.6	
308.65	1.7		316.65	2.6	
313.05	1.2		316.95	4.3	
317.40	0.7		321.00	2.0	
322.90		15.7	321.60	2.7	
323.80		1.5	322.22	3.0	
325.76	1.3		330.60	0.1	
326.08	2.1		331.20	0.9	
334.80	3.4		335.135	0.2	
338.95	0.5		339.75	2.1	
339.22		13.1	345.70		22.6
340.21	0.6		347.45	3.6	
341.25	0.8		348.00	2.9	
342.25	2.2		<b>348.78</b>	0.9	
343.60		6.3	349.20		5.5
344.05	2.7		353.95		13.9
344.36		13.9	357.12	3.5	
345.15	5.0		357.25	1.6	
347.82	7.6		358.56	2.3	
348.16	0.8		362.95	2.5	
357.00	2.9				
357.28	5.0				

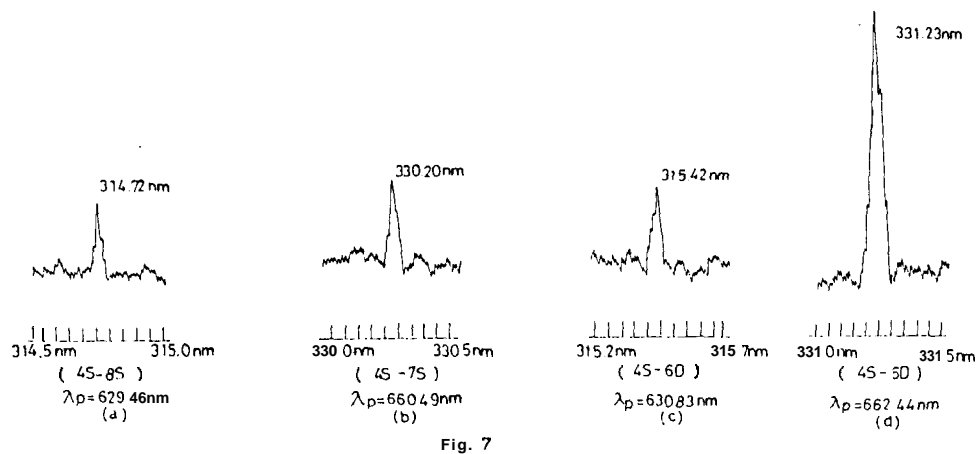


Fig. 7

FIG. 7 Spectra of frequency doubling at laser pumping wavelength (a) 629.46nm, (b) 660.49nm, (c) 630.83nm, and (d) 662.44nm.

shown in Fig. 8a. The frequency doubling spectrum at wavelength 660.00nm, which is 0.49 nm off the (4S-7S) two-photon resonance, is shown in Fig. 8b. Since the potassium vapour has inversion symmetry, the frequency doubling (a second order nonlinear process) is forbidden under the electric-dipole approximation. According to Bethune<sup>6</sup> and Okada et al.<sup>8</sup>, this process can be caused by two mechanisms in neutral atomic vapours irradiated by focused laser beams. One is due to the static electric field created by free electrons produced by multiphoton ionization, which induces frequency doubling through the third-order susceptibility  $\chi^3(2\omega; 0, \omega, \omega)$ . This induced macroscopic dc electric field, formed by the free expansion of photon-electrons around the laser beam axis, is proportional to the transversal intensity gradient of the incident laser beam. For this mechanism a finite-sized laser beam with a radial intensity gradient is necessary. The other is due to the electric-dipole-forbidden (quadrupole and magnetic dipole) second-order susceptibility. The latter

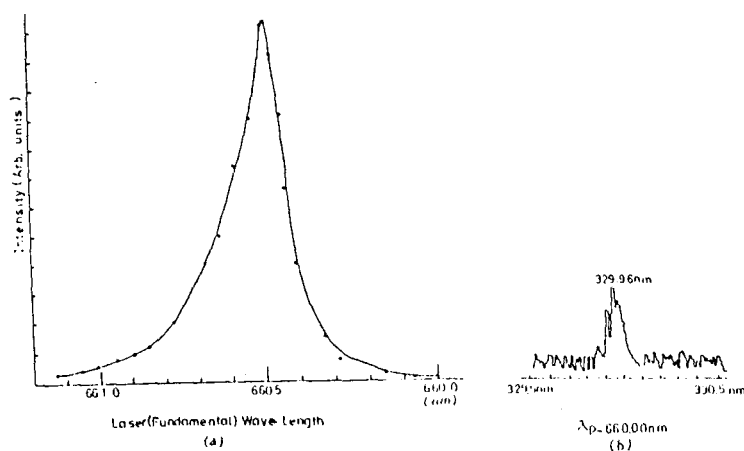


FIG. 8 Near (4S-7S) two-photon resonance (a) the frequency doubling output as a function of wavelength and (b) the frequency doubling spectrum at wavelength 660.00nm.

TABLE 7 Noncollinear Phase Matching Angles for Each UV Lines Under (4S,6D) Two-Photon Resonance

Experimental (nm) $\lambda$	Phase Matching Angle (brad)	
	$\psi$	$\phi$
308.68	2.9	
309.38	1.8	
313.05	1.8	
317.35	0.5	
319.40	1.5	
323.58	0.9	
330.48	2.8	
337.15		5.4
337.23	5.6	
338.64	1.3	
339.20	2.4	
340.22		3.8
345.32	1.7	
348.00		1.6
348.12	2.2	
348.80		10.1
352.40		0.4
353.40	4.5	
357.40	5.5	
358.71		5.5
359.40		4.1
365.14	2.1	
365.45	0.5	
369.48	4.2	
363.74	9.4	

TABLE 8 Noncollinear Phase Matching Angles for Each UV Lines Under (4S,5D) Two-photon Resonance

Experimental (nm) $\lambda$	Phase Matching Angle (brad)	
	$\psi$	$\phi$
306.78	4.4	
316.10	5.0	
320.88	1.9	
321.20	0.9	
321.54	3.9	
321.60	3.0	
321.81	3.4	
330.35	0.5	
331.23	0.1	
335.10		1.5
339.85	2.1	
342.85	4.9	
346.60	5.2	
349.15	4.2	
358.42	5.2	
368.00	3.4	

mechanism can be rejected in our experiment because we observed the same intense frequency doubling signals at (4S-7S) and (4S-8S) resonances as at the (4S-6D) resonance and it is known that all multipole transitions for S-S are strictly forbidden.

From Fig. 7, we find that the frequency doubling signal at the (4S-5D) resonance is much stronger than for the others. Actually, this line consists of two lines, one is from the frequency doubling process and the other is from a six-wave mixing process with a threefold resonant enhancement, see Table 4. The separation between the two lines is too small to be resolved in our experiment. In this case, the frequency doubling can be checked by tuning the laser off the (4S-5D) two-photon resonance where we find that the frequency doubling signal still exists but the six-wave mixing signal disappears.

#### IV. CONCLUSIONS

The generation of coherent UV lines in the wavelength range 300 to 370nm by two-photon resonant four-wave and six-wave mixing processes using potassium states  $8^2S_{1/2}$ ,  $7^2S_{1/2}$ ,  $6^2D_{3/2,5/2}$  and  $5^2D_{3/2,5/2}$  is presented. The relative intensity of the spectral lines can be explained by the resonant and near-resonant enhancements. In these multi-wave mixing processes the phase match condition can be easily satisfied by: (a) increasing the

pump laser intensity to reduce the relative collinear mismatch  $k/g$ , ; (b) tighter focussing connected with increasing divergence of the laser beam, achieving non-collinear phase match.

The frequency doubling in the potassium vapour with inversion symmetry has been observed – this can be explained by the laser induced dc electric field. The frequency doubling in the potassium vapour will be discussed in our future paper.

This project was supported by the Foundation of Defence Industry Development.

#### REFERENCES

1. W. Hartig, *Appl. Phys.* 15,427 (1978).
2. P.L. Zhang, Y.C. Wang, and A.L. Schawlow, *J. Opt. Soc. Am. B.* 1, 9 (1984).
3. A. V. Smith and J. F. Ward, *IEEE J. Quant. Elec.* QE-17, 525 (1981).
4. C. R. Vidal and F. B. Haller, *Rev. Sci. Instr.* 42, 1779 (1971).
5. A. Lindgard and S. E. Nielsen, "Atomic Data and Nuclear Data Tables" 19, No. 6, 596 (1977).
6. D. S. Bethune, *Phys. Rev. A*23, 3 139 (1981).
7. S. Bashkin and J. O. Stoner, Jr., "Atomic Energy-Level & Grotrian Diagrams" , Vol. 2, p. 280 (North-Holland, Amsterdam, 1978).
8. J. Okada, Y. Fukuda and M. Matsuoka, *J. Phys. Soc. Japan*, Vol. 50, 1301 (1981).
9. D. C. Thompson, M. S. O' Sullivan, B. P. Stoicheff, and G. X. Xu, *Can J. Phys.* 61, 949 (1983).